

Bidisperse Pore Diffusion Model for Zeolite Pressure Swing Adsorption

S. J. Doong and R. T. Yang

Department of Chemical Engineering
State University of New York
Buffalo, NY 14260

The published theoretical models for pressure swing adsorption (PSA) are of either the equilibrium type, i.e., instantaneous equilibrium is assumed between the gas and adsorbed phases, or the diffusion type considering only a monodisperse pore structure (Yang and Doong, 1985; Doong and Yang, 1987). There is reason for doubt that either type of model is applicable to adsorption processes using zeolite sorbent, which has a bidisperse pore structure. Commercial zeolite sorbents contain crystals of the size 1–9 microns that are pelletized with a binder. Sorption is entirely within the crystals, which contain micropores, whereas the binder contains macropores with a negligible sorption capacity.

This paper presents a general PSA model for zeolite sorbents. Both micropore and macropore diffusion are considered. The mathematical complexity of the pore diffusion equations for the two types of pores is reduced by assuming parabolic concentration profiles in both crystals and pellets. Thus the two partial differential equations are converted into ordinary differential equations containing only time derivatives, and the burden of integration along the radial distance is completely eliminated. The model is general enough to be applied to bulk, multicomponent separations using any PSA cycle. The specific separation discussed in this work is the bulk separation of a hydrogen-methane mixture using 5A zeolite. The boundary conditions in the model depend on the PSA cycle. A wide variety of PSA cycles has been commercialized (Yang, 1987). Under consideration here is the most widely used five-step cycle in which each adsorber undergoes the following:

- I. Repressurization with the light product
- II. High-pressure feed
- III. Cocurrent depressurization
- IV. Countercurrent blowdown
- V. Low-pressure purge.

The model is formulated for an n -component mixture. The assumptions made in the model are:

- Ideal gas behavior
- Negligible pressure drop across the bed

- Thermal equilibrium between the gas flow and the solid sorbent

- No radial temperature and concentration gradients in bed
- Spherical pellets and crystals

The dimensionless mass balance equations for the gas flow in the bed are, respectively, for the individual component and for the mixture (Doong, 1986):

$$\epsilon \frac{\partial Y_i}{\partial \tau} + U \frac{\partial Y_i}{\partial Z} + \frac{\rho_b \bar{T}}{\rho_p \bar{P}} Y_i \sum_j^n \bar{S}_j \beta_j y_{jo} - \beta_i \frac{\rho_b \bar{T}}{\rho_p \bar{P}} \bar{S}_i = 0$$

$$i = 1, 2, \dots, (n-1) \quad (1)$$

$$\frac{\partial U}{\partial Z} - \frac{\epsilon}{\bar{T}} \frac{\partial \bar{T}}{\partial \tau} - \frac{U}{\bar{T}} \frac{\partial \bar{T}}{\partial Z} - \frac{\rho_b \bar{T}}{\rho_p \bar{P}} \sum_j^n (\bar{S}_j y_{jo} \beta_j) + \epsilon \frac{\partial \bar{P}}{\partial \tau} \frac{1}{\bar{P}} = 0 \quad (2)$$

If molecular diffusion is assumed to be dominant in the binder phase of zeolite, the mass balance equations for the macropores will be similar to those for the monodisperse pore structure in Yang and Doong (1985). The resulting dimensionless equations are:

$$\frac{\partial \bar{Y}_{ip}}{\partial \tau} = \frac{1}{\bar{P}} (Y_{ip}^s - \bar{Y}_{ip}) \frac{\partial \bar{P}}{\partial \tau} - \frac{1}{\bar{T}} (Y_{ip}^s - \bar{Y}_{ip}) \frac{\partial \bar{T}}{\partial \tau} + \frac{1}{\alpha} (Y_{ip}^s - \bar{Y}_{ip}) \beta_i - \frac{\eta_i \bar{T}}{\alpha \bar{P}} \frac{\partial \bar{Q}_i}{\partial \tau} + \frac{Y_{ip}^s \bar{T}}{\alpha \bar{P}} \sum_j^n \left(y_{jo} \eta_j \frac{\partial \bar{Q}_j}{\partial \tau} \right) \quad (3)$$

$$\frac{\partial \bar{Q}_i}{\partial \tau} = 3 \int_0^1 \frac{\partial \bar{Q}_i}{\partial \tau} \left(\frac{r_p}{a_p} \right)^2 d \left(\frac{r_p}{a_p} \right) \quad (4)$$

where

$$\beta_i = \frac{L}{u_o} \frac{15}{a_p^2} D_{im}, \quad \eta_i = \frac{\rho_p q_{io}}{y_{io}} \frac{RT_o}{P_o} \quad (5)$$

Since the crystals account for all of the adsorbed amount, the first overbar on Q denotes the volume-averaged amount adsorbed over the crystal, and the second overbar denotes that averaged over the pellet. The mole fraction on the surface of the pellet Y_{ip}^s is the same as that in the bulk flow, Y_i , since the film resistance is negligible.

The local adsorption rate, \bar{S}_i , through which the bulk flow mass balance and the pore phase mass balance equations are coupled, is:

$$\bar{S}_i = -\frac{\bar{P}}{\bar{T}}(Y_{ip}^s - \bar{Y}_{ip}) - \frac{Y_{ip}^s}{\beta_i} \sum_j \left(y_{jo} \eta_j \frac{\partial \bar{Q}_j}{\partial \tau} \right) + \frac{\alpha}{\beta_i} Y_{ip}^s \frac{\bar{P}}{\bar{T}^2} \frac{\partial \bar{T}}{\partial \tau} - \frac{\alpha}{\beta_i} \frac{Y_{ip}^s}{\bar{T}} \frac{\partial \bar{P}}{\partial \tau} \quad (6)$$

Mass balance in the micropores in the crystal gives:

$$\frac{\partial q_i}{\partial t} = \frac{D_i}{r_c^2} \frac{\partial}{\partial r_c} \left(r_c^2 \frac{\partial q_i}{\partial r_c} \right) \quad (7)$$

Here, the classical Fickian law is used for crystal diffusion, as a homogeneous structure is assumed such that there is no distinction between micropores and solid walls.

By assuming a parabolic concentration profile within the crystal, the following equation is obtained:

$$\left(\frac{\partial q_i}{\partial r_c} \right)_{r_c=a_c} = \frac{5}{a_c} (q_i^s - \bar{q}_i) \quad (8)$$

Upon integration of Eq. 7 and substituting into Eq. 8, we get (in dimensionless form):

$$\frac{\partial \bar{Q}_i}{\partial \tau} = \gamma_i (Q_i^s - \bar{Q}_i), \quad \bar{Q}_i = \bar{Q}_i(r_p/a_p, Z, \tau) \quad (9)$$

where

$$\gamma_i = \frac{L}{u_o} \frac{15}{a_c^2} D_i$$

or the familiar linear driving force (LDF) approximation (Liaw et al., 1979). For macropore diffusion, the assumption of parabolic concentration profile leads to a different expression, Eq. 3, due to the accumulation in the void fraction. The usefulness of the LDF approximation has been examined for various flow conditions by Glueckauf (1955) and for a batch system by Do and Rice (1986), and a detailed discussion of the parabolic profile and LDF assumptions has been given by Yang (1987). The parabolic profile assumption is not good for rapid PSA cycles.

The dimensionless form of the heat balance equation is

$$\frac{\partial \bar{T}}{\partial \tau} + \delta_1 U \frac{\partial \bar{T}}{\partial Z} - \sum_j \left(\delta_{2j} \frac{\partial \bar{Q}_j}{\partial \tau} \right) + \delta_3 (\bar{T} - \bar{T}_w) = 0 \quad (10)$$

where

$$\delta_1 = \frac{\rho_g C_{pg}}{\epsilon \rho_g C_{pg} + \rho_b C_{pg} \sum_j (\bar{Q}_j q_{jo}) + \rho_b C_{ps}} \quad (10a)$$

$$\delta_{2i} = \frac{\rho_b q_{io} H_i \delta_i}{\rho_g C_{pg} T_o}, \quad \delta_3 = \frac{2h}{R_b \rho_g C_{pg}} \quad (10b)$$

The heat capacity of the wall is not negligible in the experimental unit. Therefore, an energy balance equation for the wall is required:

$$\frac{\partial \bar{T}_w}{\partial \tau} = \delta_4 (\bar{T} - \bar{T}_w) - \delta_5 (\bar{T}_w - 1) \quad (11)$$

where

$$\delta_4 = \frac{2h\pi R_b L}{\rho_w C_{pw} A_w u_o}, \quad \delta_5 = \frac{2h_o R_o L}{\rho_w C_{pw} A_w u_o}$$

δ_4 is for the heat transfer between the column and the wall, δ_5 is for that from the column to the ambient air.

The required input information is given in Table 1. Pure-sorbate diffusivity for CH₄ in 5A zeolite is taken from Ruthven and Derrah (1972). That for H₂ is calculated assuming Graham's law. (This assumption is not important since later results will show that the separation does not depend on H₂ diffusivity.) The macropore (1,700 Å or 170 nm) diffusivities are calculated using a tortuosity of the 4 (Ma and Ho, 1974). The void fraction in the pellet is 0.615. The heat transfer coefficients are calculated as shown previously (Yang and Doong, 1985).

The inclusion of the micropore diffusion, Eq. 7, renders the system of equations stiff, and a long computation time would be necessary for an accurate solution if the simple Euler's method were used. Thus, Eqs. 1, 2, 3, 4, 9, and 10, which form a set of simultaneous ordinary differential equations for each cell in the bed, are solved by using the GEAR method (Gear, 1971). The end condition in the bed for each cycle is used as the initial condition for the next cycle. Cyclic steady state is reached after approximately ten cycles starting from clean beds.

A further simplification can be made for Eqs. 4 and 9. They can be combined into one by assuming that Eq. 9 may be integrated with respect to the pellet radius r_p/a_p to yield:

$$\frac{\partial \bar{Q}_i}{\partial \tau} = \gamma_i (\bar{Q}_i^s - \bar{Q}_i), \quad \bar{Q}_i = \bar{Q}_i(Z, \tau) \quad (12)$$

This is true for a linear adsorption isotherm. For nonlinear isotherms, it proved to be a very good approximation, because our simulation showed very little difference between the results

Table 1. Equilibrium Adsorption Parameters, Heats of Adsorption, and Diffusivities for H₂ and CH₄ in 5A Zeolite

	CH ₄	H ₂
K_1 , mol/g sorbent	5.85×10^{-3}	6.82×10^{-3}
K_2 , mol/g · K	8.27×10^{-6}	1.48×10^{-5}
K_3 , l/kPa	5.31×10^{-6}	5.27×10^{-5}
K_4 , K	1,754.8	118.1
H_i , kJ/mol	20.72	10.05
D_o , cm ² /s	7.2×10^{-8}	2.7×10^{-7}
E , kJ/mol	12.56	12.56
$q_i = q_{mi} B_i y_i / (1 + \sum B_j P y_j); D = D_o e^{-E/RT}$		
$q_{mi} = K_1 + K_2 T; B_i = K_3 \exp(K_4/T)$		

of Eqs. 4, 9, and 12. It also reduces the number of equations in the GEAR routine because \bar{Q}_i is needed instead of \bar{Q}_i . As a result of this assumption, the computation time is reduced by a factor of three.

Comparison of Experiment and Model

Experiments were performed for the bulk separation of a 50/50 mixture of H_2 and CH_4 , with the goal of producing a high-purity H_2 . A seven-minute cycle was employed. The experimental apparatus and the operating procedure were essentially identical to those described previously (Yang and Doong, 1985; Doong and Yang, 1986). The zeolite sorbent was Linde type 5A in the form of cylindrical pellets. The diameter of the pellets was $\frac{1}{16}$ in. (0.1587 cm), which was equivalent to a hydraulic radius of 0.092 cm for spherical pellets (Antonson and Dranoff, 1969). The average crystal radius was 2 μm . The adsorber column was 2.05 cm inside radius and 60 cm long, and was packed with 610 g of pellets. The ambient temperature was 20°C. The sorbent was activated at 350°C prior to the PSA experiment. The cyclic steady state data on the effluent composition are given along with the pressure history in Figure 1.

Another model of interest is the equilibrium model, in which all mass transfer resistances are neglected (Doong and Yang, 1986). The predictions for the steady state PSA effluent composition by the equilibrium model are also shown in Figure 1. The comparison clearly shows the advantage of the pore diffusion model, and the importance of the diffusion resistances. The diffusion resistances prevent rapid uptake and cause an early breakthrough of methane. The equilibrium model predicts late and sharp breakthroughs and consequently the best separation. The difference between the predictions for steps IV and V by the two models is small. Step IV is a rapid pressure-changing step during which the flow caused by a rapid pressure drop in the

pores appears to dominate the results. This flow is accounted for in both models by using the ideal gas law. Furthermore, the pore diffusion resistance seems to be unimportant in the low-pressure purge step.

Figure 2 shows the temperature histories at three locations in the bed during a steady state PSA cycle. The experimental values were recorded by three thermocouples inserted in the bed. A peak in Figure 2 indicates the thermal wave front associated with adsorption; a trough indicates a region where desorption occurs. The major features and the magnitudes of temperature variations are adequately predicted by the pore diffusion model. However, the assumption made on the instantaneous thermal equilibrium between the gas and solid appeared to have given rise to the premature arrival of the thermal wave front, as seen in Figure 2.

Relative Importance of Micropore and Macropore Diffusion in PSA

To assess the relative importance of the macropore and micropore diffusion in zeolite PSA, the bidisperse model is applied to the $CH_4/H_2/5A$ system with various combinations of crystal and pellet sizes. The model simulation results are presented in Figure 3 as the effluent composition during the steady state PSA cycle for five different combinations of crystal and pellet sizes, as well as the results from the equilibrium model. The separation results are summarized in Table 2. The effluent velocity during step II, u_o , is kept the same for all runs, and all other conditions are nearly equal.

The results given in Figure 3 clearly demonstrate the dominance of the crystal diffusion resistance. Changing the pellet size does not appreciably influence the separation, whereas the

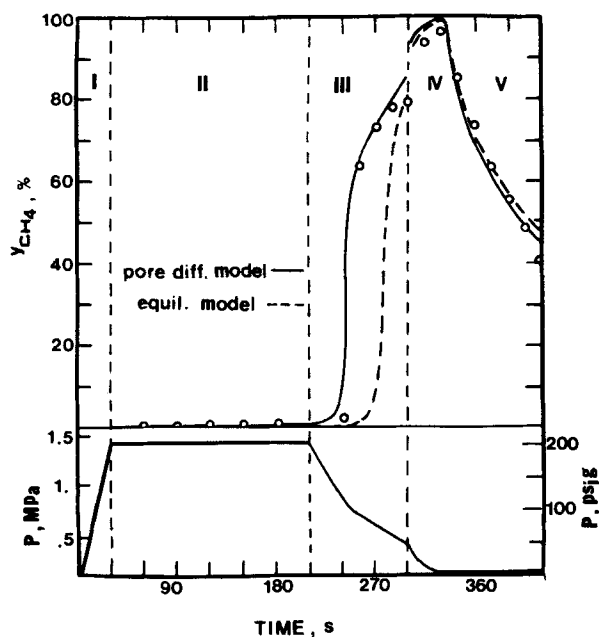


Figure 1. CH_4 concentrations in effluent in a steady state PSA cycle separating a 50/50 H_2/CH_4 mixture.
° experiment

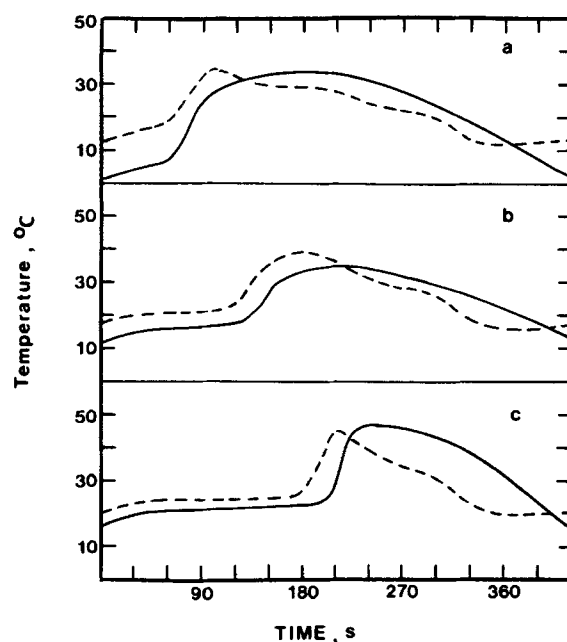


Figure 2. Temperature at various distances from feed end of bed in steady state PSA cycle of Figure 1.

a. 15.2 cm; b. 30.4 cm; c. 45.7 cm
— experiment, ---- model

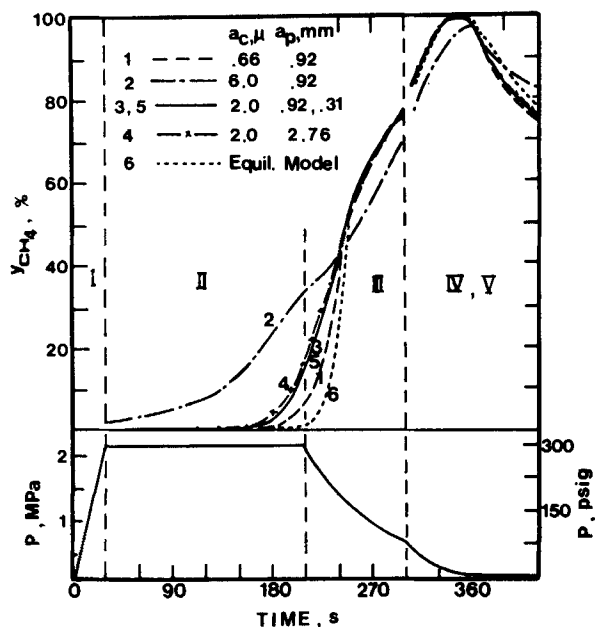


Figure 3. Effluent composition in a steady state PSA cycle separating 50/50 H₂/CH₄ using 5A zeolite with various crystal and pellet sizes.

separation is strongly affected by varying the crystal size. A crystal radius of 0.66 μm (run 1) yields results near that predicted by the equilibrium model. The commercial sorbent is simulated by run 3, with a crystal radius of 2 μm . From the simulation results, it is seen that the crystal radius of 2 μm is in a region where larger sizes will result in substantially worse separations, and a further decrease of the size does not improve the separation appreciably. However, if an ultrahigh-purity H₂ is the desired product, the equilibrium model can give a good prediction.

A semiempirical criterion has been proposed (Ruckenstein et al., 1971; Garg and Ruthven, 1974) for evaluating the relative importance of micropore and macropore diffusion for constant-pressure adsorber dynamics. The criterion is based on the magnitude of the following dimensionless group:

$$\beta = \frac{w(1 - \epsilon)}{\epsilon} \left(\frac{D_i/a_c^2}{D_{im}/a_p^2} \right) \left(\frac{dq}{dC} \right)$$

For adsorber breakthrough behavior, micropore resistance is dominant when β is significantly less than 1; when $\beta > 100$, macropore resistance controls. For the above six simulation runs for PSA separation, the β values vary widely but are in the range of 0.1 to 10 during the major portions of the runs. These β values would indicate that micropore and macropore resistances are about equal in importance. However, the micropore resistance is shown to be dominant in PSA. This can be attributed to the pressure-changing steps in the PSA cycle. During the pressure-changing steps, the convective flow in the macropore is large, whereas no such flow is assumed to occur in the crystals. As a result, the mass transfer rate in the macropores is substantially higher in the PSA cycle than that in a constant-pressure adsorber. Thus, for PSA, the value of β for macropore control is considerably higher than that for constant-pressure adsorbers. The exact values depend on the PSA process conditions, and can be determined only by using the bidisperse pore-diffusion model.

Acknowledgment

This work was supported by the Department of Energy, DE-AC21-85MC22060.

Notation

- a_c = radius of crystal, cm
- a_p = radius of pellet, cm
- C_{pg} = heat capacity of gas, J/mol/K
- C_{ps} = heat capacity of solid, J/mol/K
- D_{im} = effective macropore diffusivity, cm²/s

Table 2. Steady State PSA Predictions by Bidisperse Pore-Diffusion and Equilibrium Models for Separating 50/50 H₂/CH₄ Mixture Using 5A Zeolite

	Run					
	1	2	3	4	5	6 (Eq.)
Pellet radius, cm	0.092	0.092	0.092	0.276	0.031	—
Crystal radius, cm	6.7×10^{-5}	6.0×10^{-4}	2.0×10^{-4}	2.0×10^{-4}	2.0×10^{-4}	—
D/a_c^2 for CH ₄ , 1/s	0.11	0.0013	0.012	0.012	0.012	—
Step II						
Effluent amt.*	26.7	26.4	26.7	26.7	26.7	27.1
H ₂ purity, %	99.4	88.4	98.5	97.7	98.6	99.4
Step III						
Effluent amt.	9.4	8.2	9.4	9.3	9.4	9.9
H ₂ purity, %	48.0	50.0	46.0	46.9	45.9	53.8
Steps IV, V						
Effluent amt.	14.4	13.1	14.4	14.4	14.4	15.2
CH ₄ purity, %	92.3	88.5	92.3	92.3	92.3	92.5
H ₂ recovery, %	90.3	92.5	89.9	89.7	90.0	96.8
CH ₄ recovery, % (steps IV, V)	68.0	60.5	67.8	68.0	67.7	72.3
Purge amt.	0.72	0.72	0.72	0.72	0.72	0.66
Total feed/cycle	39.2	38.3	39.4	39.2	39.4	39.0

*All amounts are in L, STP.

D_i = crystalline diffusivity, cm^2/s
 h, h_o = heat transfer coefficient between bed and wall, between wall and ambient air, $\text{J}/\text{cm}^2/^\circ\text{C}/\text{s}$
 H = heat of adsorption, J/mol
 L = length of the bed, cm
 n = number of components in mixture
 P = total pressure, kPa
 $\bar{P} = P/P_o$
 q = amount or equilibrium amount adsorbed, mol/g
 $Q = q/q_o$
 r_c = radial distance in spherical crystal, cm
 r_p = radial distance in spherical pellet, cm
 R = gas constant
 R_o, R_i = inside and outside bed radii, cm
 S = sorption rate, $\text{mol}/\text{cm}^3 \text{ bed}/\text{s}$
 T = temperature, K
 $\bar{T} = T/T_o$
 t = time, s
 u = superficial velocity, cm/s
 u_o = effluent velocity in step II, cm/s
 U = dimensionless velocity, u/u_o
 w = volume fraction of crystal in pellet
 y = mole fraction in gas phase
 $Y = y/y_o$
 z = distance in bed from feed end, cm
 $Z = z/L$

Greek letters

ϵ = interpellet void fraction
 α = macropore void fraction within one pellet
 ρ_b = bulk density of bed, g/cm^3
 ρ_g = gas density, g/cm^3
 ρ_p = pellet density, g/cm^3
 τ = dimensionless time, $u_o t/L$

Subscripts

i = component i
 O = feed conditions
 p = in macropores
 s = at surface conditions
 w = of the wall

Superscripts

$\bar{\bar{}}$ = volume-average over the crystal
 $\bar{}$ = volume-average over the pellet

Literature cited

- Antonson, C. R., and J. S. Dranoff, "Nonlinear Equilibrium and Particle Shape Effects in Intraparticle Diffusion-Controlled Adsorption," *AIChE Symp. Ser.*, **65** (96), 20 (1969).
 Do, D. D., and R. G. Rice, "Validity of the Parabolic Profile Assumption in Adsorber Studies," *AIChE J.*, **32**, 149 (1986).
 Doong, S. J., "Bulk Gas Separation by Pressure Swing Adsorption," Ph.D. Diss., State Univ. New York, Buffalo (1986).
 Doong, S. J., and R. T. Yang, "Bulk Separation of Multicomponent Gas Mixtures by Pressure Swing Adsorption: Pore/Surface Diffusion and Equilibrium Models," *AIChE J.*, **32**, 397 (1986).
 Garg, D. R., and D. M. Ruthven, "The Performance of Molecular Sieve Adsorption Columns: Systems with Micropore Diffusion Control," *Chem. Eng. Sci.*, **29**, 571 (1974).
 Gear, G. W., *Numerical Initial-Value Problems in Ordinary Differential Equations*, Prentice Hall, Englewood Cliffs, NJ (1971).
 Glueckauf, E., "Theory of Chromatography. 10: Formula for Diffusion into Spheres and Their Application to Chromatography," *Trans. Faraday Soc.*, **51**, 1540 (1955).
 Liaw, C. H., J. S. P. Wang, R. A. Greenkorn, and K. C. Chao, "Kinetics of Fixed-bed Adsorption—A New Solution," *AIChE J.*, **25**, 376 (1979).
 Ma, Y. H., and S. Y. Ho, "Diffusion in Synthetic Faujasite Powder and Pellets," *AIChE J.*, **20**, 279 (1974).
 Ruckenstein, E., A. S. Vaidyanathan, and G. R. Youngquist, "Sorption by Solids with Bidisperse Pore Structures," *Chem. Eng. Sci.*, **26**, 1305 (1971).
 Ruthven, D. M., and R. I. Derrah, "Transition State Theory of Zeolite Diffusion, Diffusion of CH_4 and CF_4 in 5A Zeolite," *J. Chem. Soc. Trans. I*, **68**, 2332 (1972).
 Yang, R. T., *Gas Separation by Adsorption Processes*, Butterworth, Boston (1987).
 Yang, R. T., and S. J. Doong, "Gas Separation by Pressure Swing Adsorption: A Pore Diffusion Model for Bulk Separation," *AIChE J.*, **31**, 1829 (1985).

Manuscript received May 27, 1986, and revision received Sept. 15, 1986.